Influence of connection stub parameters and valve closure time on transient measurement accuracy of a pressure transducer

Zhiyong Liu and Angus R. Simpson

ABSTRACT

Consider that a transient pressure measurement occurs at the end of the connection stub attached to a pipeline. The question arises as to whether the pressure being recorded at the end of the stub is an accurate representation of pressure in the pipeline. In this study, the influence of three parameters, including pressure transducer connection stub length, stub diameter and valve closure time, on the measurement accuracy of transient pressure is investigated through numerical simulation on a reservoir-pipe-valve-reservoir system. The results show that the larger the diameter of stub, the larger its influence both on the transient in the pipe and on measurement error; the measurement accuracy increases with an increase of the length of the stub only when the closure time of the end valve is less than the time for the water hammer wave to travel back and forth between the measurement point and the end point of stub. In contrast, when the closure time of the end valve is greater than the water hammer wave return time, the measurement accuracy will decrease with an increase of the stub length; the measurement accuracy is improved as the closure time of the end valve increases. As a result, in practice, diameter and length of connection stub for the pressure-transducer should both be selected to be as small as possible.

Key words | connection stub parameters, pressure transducer, transient measurement accuracy, valve closure time, water hammer

Zhiyong Liu (corresponding author)
School of Power and Mechanical Engineering,
Wuhan University,
Wuhan, Hubei 430072,
China
E-mail: *liuzy6107@whu.edu.cn*

Angus R. Simpson
School of Civil, Environmental and Mining Engineering,
University of Adelaide,
Adelaide, South Australia 5005,
Australia

INTRODUCTION

In the last decade, various water hammer or transient-based non-invasive pipe condition assessment methods have been developed. These include the inverse transient analysis method (Liggett & Chen 1994; Vítkovský *et al.* 2000, 2007; Kapelan *et al.* 2003; Covas & Ramos 2010; Stephens *et al.* 2013), the transient-damping method (Wang *et al.* 2002, 2005), the frequency response method (Mpesha *et al.* 2001; Ferrante & Brunone 2003; Covas *et al.* 2005; Lee *et al.* 2005, 2008, 2013; Sattar & Chaudhry 2008; Duan *et al.* 2011, 2013, 2014), and the time domain reflectometry (Brunone 1999; Lee *et al.* 2007; Gong *et al.* 2013). For all these methods, a transient is injected into the pipe system and the pressure variation at one or more points is measured using high speed pressure transducers. These measured pressure traces are then analyzed in either the time domain or the frequency domain. As a result, the transient pressure measurement accuracy is a primary prerequisite for the success of transient-based methods.

Often, when measuring a transient pressure in a pipeline, it is not possible to insert the pressure transducer such that the diaphragm of the transducer is flush with the inside of the pipe. Thus, the pressure transducer is usually installed at the end of a connection stub attached to the outside diameter of the pipeline. An example of a connection stub is shown in Figure 1 (from point B to point C). For steady state flow conditions, because there is no flow in

doi: 10.2166/ws.2018.022

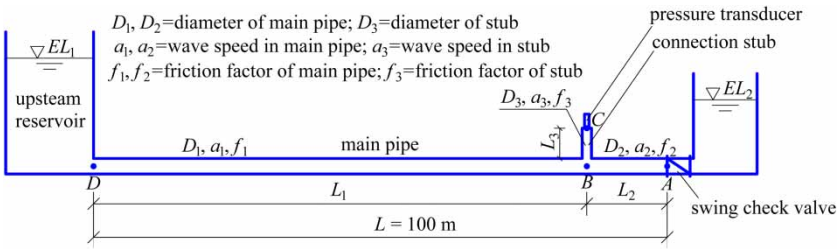

Figure 1 | Reservoir-pipe-valve-reservoir system with a pressure transducer connection stub.

the connection stub, the pressure as measured by a pressure transducer at the end of the stub (point C in Figure 1) is the same as that of the point B in Figure 1 (assuming a negligible difference in elevation). In contrast, under transient conditions, two questions now arise, including: (1) does the connection stub have an influence on the transient in the main pipe? and (2) does the pressure variation as measured at the end of the stub (point C in Figure 1) provide an accurate representation of the pressure variation in the pipeline (point B in Figure 1)?

This paper presents a series of numerical simulation results for an end-valve closure transient for the system in Figure 1 by using a method of characteristics (MOC) water hammer analysis. The influence of the dimensions of the stub (length L_3 and diameter D_3) and the closure time of the swing check valve, t_c, on the transient in the main pipe and the pressure measurement accuracy are investigated.

MATHEMATICAL MODELS

One-dimensional water hammer modeling and the MOC solution

The classical one-dimensional water hammer model comprises the unsteady pipe flow continuity equation and the unsteady momentum equation (Wylie & Streeter 1993). These equations are solved using a standard MOC formulation.

Figure 2 shows the two characteristic grids for both the main pipe and the stub in Figure 1. The first grid applies to the main pipeline where the general section is designated as *i*. The transient flow and head in the main pipeline are designated as Q_i^{main} and H_i^{main}. The second grid is for the stub and the general section is designated as *j*. The transient flow and head in the stub are designated as Q_j^{stub} and H_j^{stub}.

Along the C^+ characteristic line ($\Delta x/\Delta t = a$), the compatibility equation is:

$$H_{i,t} - H_{i-1,t-\Delta t} + \frac{a}{gA}(Q_{i,t} - Q_{i-1,t-\Delta t}) + \frac{f\Delta x}{2gDA^2} Q_{i,t}|Q_{i-1,t-\Delta t}| = 0 \quad (1)$$

or

$$H_{i,t} = C_P - B_P Q_{i,t} \quad (2)$$

where H represents the piezometric head; Q represents the flow; a is the wave speed; A is the cross sectional area of pipe; D is the diameter of pipe; t represents time; x represents the spatial coordinate along pipeline; g is the gravitational acceleration; and f represents the Darcy-Weisbach pipe friction factor; $C_P = H_{i-1,t-\Delta t} + BQ_{i-1,t-\Delta t}$; $B_P = B + R|Q_{i-1,t-\Delta t}|$; $B = a/gA, R = f\Delta x/(2gDA^2)$; Δx is the reach length; and Δt is time step.

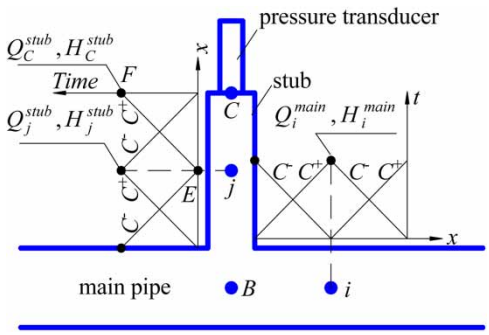

Figure 2 | The *x*-*t* plane for computation of the main pipe and stub.

Along the C^- characteristic line ($\Delta x/\Delta t = -a$), the compatibility equation is:

$$H_{i,t} - H_{i+1,t-\Delta t} - \frac{a}{gA}(Q_{i,t} - Q_{i+1,t-\Delta t}) - \frac{f\Delta x}{2gDA^2}Q_{i,t}|Q_{i+1,t-\Delta t}| = 0 \quad (3)$$

or

$$H_{i,t} = C_M + B_M Q_{i,t} \quad (4)$$

where $C_M = H_{i+1,t-\Delta t} - BQ_{i+1,t-\Delta t}$, $B_M = B + R|Q_{i+1,t-\Delta t}|$

The same equations as Equations (1)–(4) (except with the subscript j) would apply to modeling the stub.

Boundary condition of the end point of a stub

The end point of the stub (point C in Figures 1 and 2) can be considered as a dead end of the pipe. Thus, the flow at the end of the stub is $Q^{stub}_{C,t} = 0$. Consider the C^+ characteristic line from point E to point F in Figure 2. To compute the head at the stub end (point C), the C^+ compatibility equation is used:

$$H^{stub}_{C,t} = C^{stub}_P - B^{stub}_P Q^{stub}_{C,t} = C^{stub}_P \quad (5)$$

Boundary condition of the swing check valve and the downstream reservoir

The downstream end valve in the main pipeline is modeled using the dimensionless τ equation as given by Wylie and Streeter (1993) (in Example 3-1 on page 46) as:

$$\tau = \tau_i - (\tau_i - \tau_f)(t/t_c)^{EM} \quad (6)$$

The C^+ compatibility equation to the swing check valve at point A (see Figure 1) is given by:

$$H^{main}_{A,t} = C^{main}_P - B^{main}_P Q^{main}_{A,t} \quad (7)$$

The energy equation written across the valve from the upstream side at point A to the downstream reservoir (see Figure 1) is:

$$H^{main}_{A,t} - \frac{K_o}{\tau^2}\frac{Q^{main}_{A,t}\left|Q^{main}_{A,t}\right|}{A_V^2 \cdot 2g} = EL_2 \quad (8)$$

where τ is the dimensionless valve opening; τ_i is the initial valve opening; τ_f is the final valve opening; t_c is the closure time of the valve; EM is the exponent that defines the valve curve; K_o is the valve loss coefficient when the valve is fully open (the general fitting or minor head loss equation is $h_L = KV^2/2g$, where K is the loss coefficient); A_V is the cross sectional area of valve; and EL_2 is the downstream reservoir elevation.

Boundary condition of the junction between the main pipe and the stub

The boundary condition of the junction between the main pipe and the stub (see point B in Figures 1 and 2) can be expressed as:

The C^+ and C^- compatibility equations in the main pipe are:

$$H^{main}_{B,t} = C^{main}_P - B^{main}_P Q^{main}_{uB,t} \quad (9)$$

$$H^{main}_{B,t} = C^{main}_M + B^{main}_M Q^{main}_{B,t} \quad (10)$$

The C^- compatibility equation in the stub towards the junction at point B is:

$$H^{stub}_{B,t} = C^{stub}_M + B^{stub}_M Q^{stub}_{B,t} \quad (11)$$

Other required equations are as follows, including the continuity of flow at the junction:

$$Q^{main}_{uB,t} = Q^{main}_{B,t} + Q^{stub}_{B,t} \quad (12)$$

$$H^{main}_{B,t} = H^{stub}_{B,t} \quad (13)$$

where $Q^{main}_{uB,t}$ and $Q^{main}_{B,t}$ are the flows upstream and downstream, respectively, of point B in main pipe; and $Q^{stub}_{B,t}$ is the flow in the stub at the junction.

Boundary condition of upstream constant head reservoir

The boundary condition at point D (see Figure 1) is a standard constant head condition. Thus, the head at point D is $H_{D,t}^{main} = EL_1$. Along the C^- characteristic line, the boundary condition at point D can be expressed as:

$$H_{D,t}^{main} = C_M^{main} + B_M^{main} Q_{D,t}^{main} = EL_1 \quad (14)$$

where EL_1 is the upstream reservoir elevation.

System configuration

The parameters of the system defined in Figure 1 are summarized in Table 1, in which the friction factors for main pipe and stub are calculated by using Chézy formula and Manning formula, and the roughness coefficient is 0.012. It is assumed that the following holds for the system in Figure 1: $L_3 < L_2 < L_1$.

RESULTS AND DISCUSSION

Examination of the system behavior assuming the absence of a stub

In order to investigate the influence of the presence of a pressure transducer connection stub on the transient in the main pipe, the end-valve closure transient in a system is first simulated without a pressure transducer connection stub. The results will be used as the baseline for the comparison analysis as presented in the following sections.

In Figure 1, consider the system without the stub, when the end valve at point A is closed at a time of $t = 0.0$ s, a positive water hammer wave is generated and will travel back

Table 1 | System parameters for Figure 1

Symbol	Parameter	Value
L (m)	Total length of main pipe	100
L_1 (m)	Main pipe length from measurement point to upstream reservoir	90
L_2 (m)	Main pipe length from measurement point to end valve	10
L_3 (m)	Length of stub	Varies
EL_1 (m)	Upstream reservoir elevation	10.0
EL_2 (m)	Downstream reservoir elevation	8.0
$D_1 = D_2 = D$ (mm)	Main pipe diameter	1,000
D_3 (m)	Stub diameter	Varies
$f_1 = f_2$	Friction factor for main pipe	0.018
f_3	Friction factor for stub (for $D_3 = 15$ mm)	0.073
h_f (m)	Head loss in main pipe for frictional case	0.3
$a_1 = a_2 = a_3$ (m/s)	Wave speeds in main pipe and stub	1,000
V_0 (m/s)	Initial velocity for frictionless system	1.98
$V_{0\text{-}f}$ (m/s)	Initial velocity for frictional system	1.82
τ_i	Initial dimensionless valve position	1.0
τ_f	Final dimensionless valve position	0.0
EM	Exponent that defines the valve curve	1.0
K_0	Valve loss coefficient when the valve is fully open	10.0
Δx (m)	Reach length in MOC calculations	0.1
Δt (s)	Time step in MOC calculations	0.00001
t_c (s)	Time of closure of valve	Varies

and forth in the system with wave return time of $2(L_1/a_1 + L_2/a_2)$ or 0.2 s. The wave will be reflected only at point D and point A.

The simulation results of the transient pressure at point B under the condition of the absence of a connection stub (subscripted as 'WS', without stub) for different cases are presented in Table 2, in which t_0 represents the time for a water hammer wave to travel from point A to point B, $t_0 = L_2/a_2$; t_1 represents the time for a water hammer wave to travel from point B to point D and back to point B, $t_1 = 2L_1/a_1$; $H_{WS\text{-}B\max}$ represents the maximum head at point B during the period from the time of $t = 0.0$ s to a time of $t = (t_c + t_0 + t_1)$; $t_{WS\text{-}B\max}$ represents the time of occurrence of $H_{WS\text{-}B\max}$. Various swing check valve closure times as shown in Column 1 of Table 2 are simulated.

For the frictionless case, the head at point B reaches its maximum value at the time of $t = t_c + t_0$. If t_c is less than t_1 (the wave return time from point B to the upstream reservoir at point D and back to point B), the value of $H_{WS\text{-}B\max}$ is not affected by the wave reflection from point D and can be calculated by the Joukowky formula. In addition, it does not change with the change of t_c. However, if t_c is larger than t_1, a reflected wave will return from point D to point B before the velocity at point B reduces to zero. Thus, $H_{WS\text{-}B\max}$ will be less than that for the case of t_c being larger than t_1. In addition, the maximum head decreases with an increase of t_c.

For the frictional case, the value of $H_{WS\text{-}Bmax}$ decreases with an increase of the valve closure time t_c for all cases. If t_c is less than t_1, the maximum head $H_{WS\text{-}Bmax}$ will occur at the time of $t = t_0 + t_1$ rather than $t = t_c + t_0$ because of the effect of line pack. However, if t_c is larger than t_1, the maximum head will occur at time of $t = t_c + t_0$ because of the influence of the reflected wave from point D. Note that the initial velocity for the frictionless case ($V_0 = 1.98$ m/s) is less than the initial velocity for the frictional case ($V_0 = 1.82$ m/s). These velocities were calculated based on the fully open valve loss coefficient of $K_o = 10.0$ as shown in Table 1.

Influence of the ratio of the stub diameter to the main pipe diameter (D_3/D) on the transient in the main pipe

In Figure 1, when the valve at the end of the pipe is closed at a time of $t = 0.0$ s, a positive water hammer wave, W_0, is generated and travels from point A in the upstream direction. At a time of $t_0 = L_2/a_2$ s, the water hammer wave reaches point B and splits into three parts at the junction B, i.e. waves W_1, W_2 and W_3. Wave W_1 will continue traveling upstream from point B towards the constant head reservoir at point D and is reflected back towards point B where it arrives after $t_1 = 2L_1/a_1$ s. Meanwhile, wave W_2 is reflected back towards

Table 2 | Simulation results of the transient pressure at point B in Figure 1 (without stub)

	Frictionless ($V_0 = 1.98$ m/s)				With friction ($f_1 = f_2 = 0.018$, $V_0 = 1.82$ m/s)			
t_c (s) Col. (1)	$H_{WS\text{-}B}$ at $t = (t_c + t_0)$ (m) Col. (2)	$H_{WS\text{-}Bmax}$ (m) Col. (3)	$t_{WS\text{-}Bmax}$ (s) Col. (4)	Formula for calculation of $t_{WS\text{-}Bmax}$ Col. (5)	$H_{WS\text{-}B}$ at $t = (t_c + t_0)$ (m) Col. (6)	$H_{WS\text{-}Bmax}$ (m) Col. (7)	$t_{WS\text{-}Bmax}$ (s) Col. (8)	Formula for calculation of $t_{WS\text{-}Bmax}$ Col. (9)
0.0	212.03	212.03	0.01	$t_c + t_0$	195.76	196.03	0.19	$t_0 + t_1$
0.0005	212.03	212.03	0.0105	$t_c + t_0$	195.76	196.03	0.19	$t_0 + t_1$
0.001	212.03	212.03	0.011	$t_c + t_0$	195.76	196.03	0.19	$t_0 + t_1$
0.003	212.03	212.03	0.013	$t_c + t_0$	195.76	196.03	0.19	$t_0 + t_1$
0.005	212.03	212.03	0.015	$t_c + t_0$	195.76	196.03	0.19	$t_0 + t_1$
0.01	212.03	212.03	0.02	$t_c + t_0$	195.76	196.02	0.19	$t_0 + t_1$
0.05	212.03	212.03	0.06	$t_c + t_0$	195.77	195.97	0.19	$t_0 + t_1$
0.1	212.03	212.03	0.11	$t_c + t_0$	195.78	195.91	0.19	$t_0 + t_1$
0.2	211.57	211.57	0.21	$t_c + t_0$	195.42	195.42	0.21	$t_c + t_0$
0.5	189.04	189.04	0.51	$t_c + t_0$	176.26	176.26	0.51	$t_c + t_0$
1.0	129.76	129.76	1.01	$t_c + t_0$	124.17	124.17	1.01	$t_c + t_0$

point A and will return to point B again after $t_2 = 2L_2/a_2$ seconds after being reflected from the downstream end valve. Finally, wave W_3 will repeatedly travel in the connection stub back and forth between point B and point C with a return time of $t_3 = 2L_3/a_3$ seconds. The waves traveling back and forth in the stub will interact with the waves traveling in the main pipe and it will be difficult to separate the effect of each wave. Superposition of these various water hammer waves in the main pipe and stub can only be determined using a MOC model.

In order to simplify the analysis and analyze the influence of a connection stub on the transient in the main pipe, the end valve is assumed to close instantaneously (the valve closure time will be varied later on in the paper) and the analysis time is limited to the period from $t = 0.0$ s to a time of $t = (t_c + t_0 + t_2)$ s for this system to ensure there is no influence from waves W_1 and W_2. Moreover, in this section, in order to highlight the influence of the ratio of the stub diameter to the diameter of the main pipe (D_3/D), the system is assumed to be frictionless in both the main pipe and the connection stub. The friction will be considered when discussing the influence of the stub length and the valve closure time in the following sections.

The simulation results for influence of D_3/D on transient head at point B are shown in Table 3, in which t_4 represents the time of the valve closure time plus the time for a water hammer wave to travel from the valve to the junction B, $t_4 = t_c + t_0$; t_5 represents the time of the valve closure time plus the time for a water hammer wave to travel from the valve to the junction B and then up the stub to point C and back to the junction B, $t_5 = t_c + t_0 + t_3$.

The heads at point B for two cases, H_{WS-B} (for the case of without the presence of a connection stub) and H_B (for the case of with the presence of a stub), are compared at a time of $t = t_4$ and $t = t_5$. A variable, $Err_{B\text{-}B(ws)}$, representing the percentage difference between H_{WS-B} and H_B, is defined as follows: $Err_{B-B(WS)} = (H_B - H_{WS-B})/H_{WS-B} \times 100\%$.

In Table 3, at a time of $t = t_4$, the head at point B is reduced as a result of the presence of the stub (see Column 8 in Table 3). The reduction of head increases markedly as the size of the stub increases to be the same order as the diameter of the main pipe (in Column 6, a change occurs down the column from a value of 212.01 m to 144.69 m for both a 100 mm and 1.0 m stub length as the stub diameter changes from 15 mm to 1.0 m). Because the system is assumed to be frictionless, the length of the stub has no influence on the head at point B at the time of $t = t_4$. These head values compare with 212.03 m for the case of no stub.

Now consider the condition where the wave has traveled along the stub, reflected from point C (which is a dead end), and returned back to point B at a time of $t = t_5$.

Table 3 | Influence of D_3/D on transient head of point B ($f = 0.0$, $t_c = 0.0$)

			Without connection stub H_{WS-B} (m)		With connection stub H_B(m)		$Err_{B\text{-}B(WS)}$(%)	
L_3 (m) Col. (1)	D_3 (mm) Col. (2)	D_3/D Col. (3)	At $t = t_4$ Col. (4)	At $t = t_5$ Col. (5)	At $t = t_4$ Col. (6)	At $t = t_5$ Col. (7)	At $t = t_4$ Col. (8)	At $t = t_5$ Col. (9)
0.1	15	0.015	212.03	212.03	212.01	212.05	−0.01	0.01
	20	0.02	212.03	212.03	211.99	212.07	−0.02	0.02
	50	0.05	212.03	212.03	211.78	212.28	−0.12	0.12
	100	0.1	212.03	212.03	211.03	213.03	−0.47	0.47
	200	0.2	212.03	212.03	208.07	215.84	−1.87	1.80
	500	0.5	212.03	212.03	189.58	229.49	−10.59	8.23
	1,000	1	212.03	212.03	144.69	234.48	−31.76	10.59
1.0	15	0.015	212.03	212.03	212.01	212.05	−0.01	0.01
	20	0.02	212.03	212.03	211.99	212.07	−0.02	0.02
	50	0.05	212.03	212.03	211.78	212.28	−0.12	0.12
	100	0.1	212.03	212.03	211.03	213.03	−0.47	0.47
	200	0.2	212.03	212.03	208.07	215.84	−1.87	1.80
	500	0.5	212.03	212.03	189.58	229.49	−10.59	8.23
	1,000	1	212.03	212.03	144.69	234.48	−31.76	10.59

The head at point B is now greater than the head for the case of without the stub (see Column 9 in Table 3). In addition, the length of the stub has no influence on the head at point B at the time of $t = t_5$. In Column 7, a change occurs from a value of 212.05 m to 234.48 m for both a 100 mm and 1.0 m stub length as the stub diameter changes from 15 mm to 1.0 m. Thus, at a time of t_5, the head in the connector stub is larger than the head in the main pipe. The larger the stub diameter ratio value of D_3/D, the more energy the connector stub has, and the more influence it has on the head of point B.

The results of Columns 8 and 9 in Table 3 are plotted in Figure 3.

From the above analysis, it has been found that the larger the value of D_3/D, the larger the influence of the connector stub on the transient in the main pipe. So in order to decrease this influence, the value of stub diameter D_3 should be as small as practicable. Since $D_3 = 15$ mm is typically the smallest size that one would expect in usual engineering applications, this stub diameter value is now selected for the following analysis.

Influence of connection stub length on transient pressure measurement accuracy

In order to analyze the influence of the length of the connection stub, L_3, on the transient pressure measurement accuracy, the transient for the case of a stub diameter of $D_3 = 15$ mm is simulated for two different conditions. The first condition is for a valve closure time of less than $2L_3/a_3$, while the other condition is for a valve closure time of larger than $2L_3/a_3$.

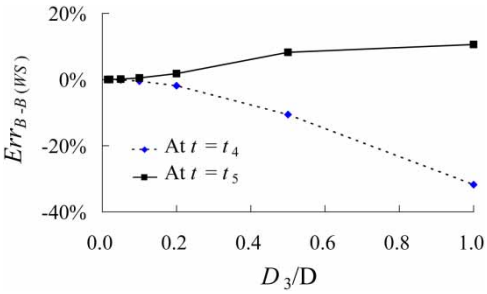

Figure 3 | Influence of the value D_3/D on the head at point B relative to a system without a connection stub ($f = 0$, $t_c = 0$).

Case of a valve closure time less than $2\,L_3\,/a_3$ seconds

Consider the case where a stub diameter, D_3, is 15 mm, the closure time of the end valve, t_c, is 0.0 s, and the shortest stub length, L_3, is 0.02 m. Thus, t_c is less than $2L_3/a_3 = 0.00004$ s ($a_3 = 1{,}000$ m/s, as shown in Table 1).

The simulation results for the case assuming zero friction and for a frictional condition with the stub length L_3 varying from 0.02 m to 1.0 m are shown in Table 4, in which $H_{C\max}$ represents the maximum head at point C for the situation of the presence of a stub during the period from a time of $t = 0.0$ to the time of $t_5 = (t_c + t_0 + t_3)$ for this system; $H_{WS\text{-}B\max}$ represents the maximum head at point B under the condition of no stub; $t_{C\max}$ represents the time of occurrence of $H_{C\max}$; $Err_{C\text{-}B(ws)}$ represents the percentage difference between $H_{WS-B\max}$ and $H_{C\max}$, and is defined as follows: $Err_{C-B(WS)} = (H_{C\max} - H_{WS-B\max})/H_{WS-B\max} \times 100\%$.

For the frictionless case, $H_{C\max}$ and $Err_{C\text{-}B(ws)}$ for all the cases of different stubs lengths in Table 4 are the same. Thus, they are not influenced by the stub length L_3. The water hammer wave that travels along the stub from point B to point C reflects from the dead end at point C and causes a very significant increase in head ($H_{C\max}$ reaches 414.02 m – compared to a value of 212.03 m at point B for the case with no stub present). The time at which the maximum head at point C occurs, $t_{C\max}$, is given in Column 5 in Table 4.

For frictional case, $H_{C\max}$ and $Err_{C\text{-}B(ws)}$ are the same for the cases of stubs lengths of 0.02 m, 0.05 m and 0.1 m. While both $H_{C\max}$ and $Err_{C\text{-}B(ws)}$ decrease with an increase of the length of the stub L_3, when the length of the stub is longer than 0.1 m. This is because the larger the stub length L_3, then the larger the friction loss in the stub. And when the length of the stub is less than 0.1 m, the influence of the friction loss on transient pressure in the stub is almost the same. For example, compare the three cases where the stub length L_3 is 0.02 m, 0.1 m and 1.0 m, respectively. The maximum head at point C at the end of the connection stub, $H_{C\max}$ is 381.75 m, 381.75 m and 381.02 m, respectively. In contrast, for the case without a connection stub, the head at point B, $H_{WS\text{-}B\max}$, is 196.03 m. Thus, the percentage differences of head of $Err_{C\text{-}B(ws)}$ are 94.74%, 94.74% and 94.37%, respectively, for these three lengths. The time of $t_{C\max}$ is given in Column 5 in Table 4.

Table 4 | Simulation results for the case of a stub diameter $D_3 = 15$ mm with various stub lengths (L_3) and an instantaneous valve closure of $t_c = 0.0$ s

		With connection stub				
f Col. (1)	Without connection stub $H_{WS\text{-}Bmax}$ (m) Col. (2)	L_3 (m) Col. (3)	H_{Cmax} (m) Col. (4)	t_{Cmax} (s) Col. (5)	Formula for t_{Cmax} Col. (6)	$Err_{C\text{-}B(ws)}$ (%) Col. (7)
Frictionless	212.03	0.02	414.02	0.01002	$t_c + L_2/a_2 + L_3/a_3$	95.26
$f_1 = f_2 = f_3 = 0$		0.05	414.02	0.01005	$t_c + L_2/a_2 + L_3/a_3$	95.26
		0.10	414.02	0.01010	$t_c + L_2/a_2 + L_3/a_3$	95.26
		0.20	414.02	0.01020	$t_c + L_2/a_2 + L_3/a_3$	95.26
		0.30	414.02	0.01030	$t_c + L_2/a_2 + L_3/a_3$	95.26
		0.40	414.02	0.01040	$t_c + L_2/a_2 + L_3/a_3$	95.26
		0.50	414.02	0.01050	$t_c + L_2/a_2 + L_3/a_3$	95.26
		0.60	414.02	0.01060	$t_c + L_2/a_2 + L_3/a_3$	95.26
		0.70	414.02	0.01070	$t_c + L_2/a_2 + L_3/a_3$	95.26
		0.80	414.02	0.01080	$t_c + L_2/a_2 + L_3/a_3$	95.26
		0.90	414.02	0.01190	$t_c + L_2/a_2 + L_3/a_3$	95.26
		1.00	414.02	0.01100	$t_c + L_2/a_2 + L_3/a_3$	95.26
With friction	196.03	0.02	381.75	0.01006	$t_c + L_2/a_2 + 3L_3/a_3$	94.74
$f_1 = 0.018$		0.05	381.75	0.01015	$t_c + L_2/a_2 + 3L_3/a_3$	94.74
$f_2 = 0.018$		0.10	381.75	0.01030	$t_c + L_2/a_2 + 3L_3/a_3$	94.74
$f_3 = 0.073$		0.20	381.67	0.01060	$t_c + L_2/a_2 + 3L_3/a_3$	94.70
		0.30	381.60	0.01090	$t_c + L_2/a_2 + 3L_3/a_3$	94.66
		0.40	381.50	0.01120	$t_c + L_2/a_2 + 3L_3/a_3$	94.61
		0.50	381.42	0.01150	$t_c + L_2/a_2 + 3L_3/a_3$	94.57
		0.60	381.34	0.01180	$t_c + L_2/a_2 + 3L_3/a_3$	94.53
		0.70	381.26	0.01210	$t_c + L_2/a_2 + 3L_3/a_3$	94.49
		0.80	381.18	0.01240	$t_c + L_2/a_2 + 3L_3/a_3$	94.45
		0.90	381.10	0.01270	$t_c + L_2/a_2 + 3L_3/a_3$	94.41
		1.00	381.02	0.01300	$t_c + L_2/a_2 + 3L_3/a_3$	94.37

For the above three cases, $H_{C\max}$ is very much larger than $H_{WS\text{-}B\max}$, and the percentage difference $Err_{C\text{-}B(ws)}$ is correspondingly large, which means the measurement accuracy is very low.

Case of a valve closure time larger than $2\,L_3/a_3$ s

Consider the case in which the stub diameter, D_3, is 15 mm, the closure time of the end valve, t_c, is 0.003 s, and the shortest stub length, L_3, is 0.02 m. A small valve closure time, 0.003 s, has been selected for illustrative purposes. Thus, t_c is larger than $2L_3/a_3$ (0.00004 s) and less than both $2L_2/a_2$ (0.02 s) and $2L_1/a_1$ (0.18 s) to ensure the value of $H_{C\max}$ is not affected by waves W_1 and W_2.

The simulation results for the case assuming zero friction and for a frictional condition with stub lengths L_3 from 0.02 m to 1.0 m are shown in Table 5 and Figure 4.

For all the cases in Table 5, the valve closure time t_c is 0.003 s (3 milliseconds), which is larger than the stub water hammer wave return time of $2L_3/a_3$ (for the maximum length stub of 1.0 m in Table 5, the maximum value of $2L_3/a_3$ is 0.002 s). The maximum head at the end of the connection stub (point C) of $H_{C\max}$ will increase with an increase of stub length L_3, as depicted in Table 5, and the percentage difference $Err_{C\text{-}B(ws)}$ will also increase with an increase of stub length L_3, as depicted in Figure 4. Thus, the measurement accuracy of a transducer at point C to indicate the true pressure head at point B gets worse as the stub gets longer. Moreover, the smaller the connection stub length of L_3, then the smaller the stub water hammer wave return time of $2L_3/a_3$, thus there will be more positive and negative water hammer waves reflecting back and forth and experienced at point C before the velocity of point B reaches 0.0 m/s. As a result, the maximum head at the transducer location of $H_{C\max}$ and the percentage difference of $Err_{C\text{-}B(ws)}$ both decrease with a decrease of stub length L_3.

For the frictionless case in Table 5 and Figure 4, $H_{C\max}$ is 225.64 m, 245.73 m and 278.14 m, which overestimates the head by 6.42%, 15.89% and 31.18%, for a stub length of 0.02 m, 0.05 m and 0.1 m, respectively. While for a stub

Table 5 | Simulation results for the case of a stub diameter of $D_3 = 15$ mm for various stub lengths (L_3) and a valve closure time of $t_c = 0.003$ s

f	Without stub	With stub				
Col. (1)	$H_{WS\text{-}Bmax}$ (m) Col. (2)	L_3 (m) Col. (3)	H_{Cmax} (m) Col. (4)	t_{Cmax} (s) Col. (5)	Formula for t_{Cmax} Col. (6)	$Err_{C\text{-}B(ws)}$ (%) Col. (7)
Frictionless	212.03	0.02	225.64	0.01302	$t_c + L_2/a_2 + L_3/a_3$	6.42
$f_1 = f_2 = f_3 = 0$		0.05	245.73	0.01305	$t_c + L_2/a_2 + L_3/a_3$	15.89
		0.10	278.14	0.01310	$t_c + L_2/a_2 + L_3/a_3$	31.18
		0.20	330.01	0.01320	$t_c + L_2/a_2 + L_3/a_3$	55.64
		0.30	362.21	0.01330	$t_c + L_2/a_2 + L_3/a_3$	70.83
		0.40	379.93	0.01340	$t_c + L_2/a_2 + L_3/a_3$	79.19
		0.50	391.51	0.01350	$t_c + L_2/a_2 + L_3/a_3$	84.65
		0.60	397.47	0.01360	$t_c + L_2/a_2 + L_3/a_3$	87.46
		0.70	401.41	0.01370	$t_c + L_2/a_2 + L_3/a_3$	89.32
		0.80	404.60	0.01380	$t_c + L_2/a_2 + L_3/a_3$	90.82
		0.90	407.28	0.01390	$t_c + L_2/a_2 + L_3/a_3$	92.09
		1.00	409.23	0.01400	$t_c + L_2/a_2 + L_3/a_3$	93.01
With friction	196.03	0.02	208.81	0.01302	$t_c + L_2/a_2 + L_3/a_3$	6.52
$f_1 = 0.018$		0.05	228.07	0.01305	$t_c + L_2/a_2 + L_3/a_3$	16.34
$f_2 = 0.018$		0.10	258.97	0.01310	$t_c + L_2/a_2 + L_3/a_3$	32.11
$f_3 = 0.073$		0.20	307.44	0.01320	$t_c + L_2/a_2 + L_3/a_3$	56.83
		0.30	336.52	0.01330	$t_c + L_2/a_2 + L_3/a_3$	71.67
		0.40	352.16	0.01340	$t_c + L_2/a_2 + L_3/a_3$	79.65
		0.50	362.18	0.01350	$t_c + L_2/a_2 + L_3/a_3$	84.76
		0.60	367.28	0.01360	$t_c + L_2/a_2 + L_3/a_3$	87.36
		0.70	370.60	0.01370	$t_c + L_2/a_2 + L_3/a_3$	89.05
		0.80	373.26	0.01380	$t_c + L_2/a_2 + L_3/a_3$	90.41
		0.90	375.45	0.01390	$t_c + L_2/a_2 + L_3/a_3$	91.53
		1.00	377.04	0.01400	$t_c + L_2/a_2 + L_3/a_3$	92.34

length of 1.0 m, the value is 409.23 m which is an overestimate of head of 93.01% and considerably less accurate. The time at which the maximum head at point C occurs, t_{Cmax}, is given in Column 5 in Table 5.

For the frictional case in Table 5 and Figure 4, H_{Cmax} is 208.81 m, 228.07 m and 258.97 m, which is an overestimate of pressure head of 6.52%, 16.34% and 32.11%, for a stub length of 0.02 m, 0.05 m and 0.1 m, respectively. While for a stub length of 1.0 m, the value is 377.04 m, which again is an overestimate of pressure head of 92.34%. Thus, the influence of friction in this case is small, which is also clearly shown in Figure 4. The time of t_{Cmax} is given in Column 5 in Table 5. Often the stub length L_3 is less than 1.0 m, so $2L_3/a_3$ is less than 0.002 s and, as a result, the valve closure time t_c is usually larger than the stub return time of $2L_3/a_3$. Thus, according to analysis above, the length of the connection stub L_3 should be as small as possible to improve the measurement accuracy. Now the effect of varying the closure time of the end valve will be considered. In the following analysis, L_3 is selected as 0.02 m, 0.05 m and 0.1 m, respectively.

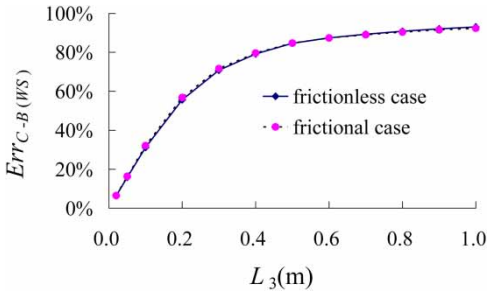

Figure 4 | Variation of relative difference between maximum heads at point C and point B with L_3 ($t_c = 0.003$ s, $D_3 = 15$ mm).

Influence of the valve closure time on the difference of the head between point B and point C

Simulation results for the cases of $D_3 = 15$ mm, $L_3 = 0.02$ m, 0.05 m and 0.1 m with different valve closure times t_c are shown in Table 6 and Figure 5.

Table 6 | Simulation results for the cases with different t_c ($D_3 = 15$ mm, friction included)

L_3 (m) Col. (1)	t_c (s) Col. (2)	$2L_3/a_3$ (s) Col. (3)	$t_c/(2L_3/a_3)$ Col. (4)	$H_{WS\text{-}B\max}$ (m) Col. (5)	$H_{C\max}$ (m) Col. (6)	$Err_{C\text{-}B(ws)}$ (%) Col. (7)
0.02	0.0	0.00004	0	196.03	381.75	94.74
	0.0001		2.5	196.03	367.59	87.52
	0.0002		5	196.03	336.60	71.71
	0.001		25	196.03	234.53	19.64
	0.002		50	196.03	215.24	9.80
	0.01		250	196.03	199.67	1.86
	0.02		500	196.01	197.72	0.87
	0.04		1,000	195.98	196.75	0.39
	0.1		2,500	195.91	196.17	0.13
	0.2		5,000	195.42	195.62	0.10
0.05	0.0	0.0001	0	196.03	381.75	94.74
	0.00025		2.5	196.03	367.59	87.52
	0.0005		5	196.03	336.60	71.71
	0.0025		25	196.03	234.53	19.64
	0.005		50	196.03	215.24	9.80
	0.025		250	196.00	199.67	1.87
	0.05		500	195.98	197.72	0.89
	0.1		1,000	195.91	196.76	0.43
	0.25		2,500	193.38	193.77	0.20
	0.5		5,000	176.26	176.44	0.10
0.1	0.0	0.0002	0	196.03	381.75	94.74
	0.0005		2.5	196.03	367.59	87.52
	0.001		5	196.03	336.60	71.71
	0.005		25	196.03	234.53	19.64
	0.01		50	196.03	215.25	9.80
	0.05		250	195.98	199.68	1.89
	0.1		500	195.91	197.75	0.94
	0.2		1,000	195.42	196.40	0.50
	0.5		2,500	176.26	176.61	0.20
	1		5,000	124.17	124.28	0.09

For the same reasons as described above, the larger the valve closure time t_c, the more times a wave will travel back and forth between point B and point C before the velocity of point B reaches 0.0 m/s. As a result, both $H_{C\max}$ and $Err_{C\text{-}B(ws)}$ decrease with an increase of the valve closure time t_c. This is clearly shown in Table 6 and Figure 5. For example, for the case of stub length of 0.1 m, when the valve closure time $t_c = 1.0$ s (which is 5,000 times the stub water hammer wave return time of $2L_3/a_3 = 0.0002$ s), then $H_{C\max}$ is 124.28 m and very close to $H_{WS\text{-}B\max}$ value of 124.17 m or an overestimate of 0.111 m or a $Err_{C\text{-}B(ws)}$ value of 0.09% which exhibits satisfactory measurement accuracy. It also can be found that under the same value of $t_c/(2L_3/a_3)$, the values of $Err_{C\text{-}B(ws)}$ are almost the same for different stub lengths; while under the same value of t_c, the value of $Err_{C\text{-}B(ws)}$ increases with the increase of stub length. Thus, as long as the valve closure time exceeds the value of 500 times the stub water hammer wave return time of $2L_3/a_3$, the pressure transducer at point C will measure the pressure variation in the main pipeline at point B with an acceptable accuracy (the percentage difference between maximum heads at point C and point B is no more than 0.94%). In the case of a swing check valve slam where the time of closure is smaller than the value of 500 times $2L_3/a_3$, one must be careful about using a transducer at the end of a connection stub (even if it is very short and has a small diameter) as the pressure head measured will differ (perhaps exceeding say 0.94% of percentage difference) from the actual pressure in the main pipeline.

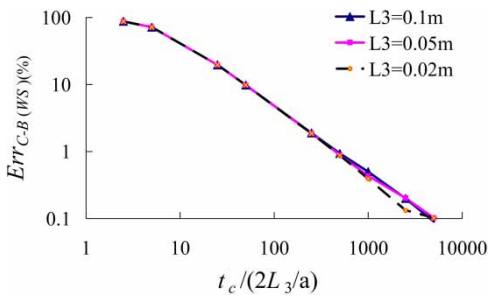

Figure 5 | Variation of relative difference between maximum heads at point C and point B with $t_c/(2L_3/a_3)$ ($D_3 = 15$ mm).

CONCLUSIONS

This paper investigates the influence of connection stub parameters and valve closure time on transient measurement accuracy of a pressure transducer in a reservoir-pipe-valve-reservoir system by using the MOC analysis.

Firstly, the influence of the ratio of the stub diameter to the main pipe diameter on the transient in the main pipe is analyzed under an assumption of zero friction. It is observed that the larger the diameter of the stub, the larger its influence on the transient in the main pipe.

Then the influence of connection stub length on the difference between transient head at the measurement point (the junction of stub and main pipe) and the end point of stub (the installing point of a transducer) is

investigated for both frictionless and frictional cases. The results show that this difference increases with an increase of the length of the stub when the closure time of the end valve is greater than the time for the water hammer wave to travel back and forth between the measurement point and the end point of stub, which means a decrease of the measurement accuracy with an increase of the stub length. In contrast, this difference decreases with an increase of the length of the stub only when the closure time of the end valve is less than the water hammer wave return time as defined immediately above.

Finally, this paper investigates the influence of the valve closure time on the difference between the transient pressure at the measurement point and the end point of stub. The results show that this difference decreases with an increase of the closure time of the end valve, which means an improvement of the measurement accuracy with an increase of the closure time of the end valve.

In practice, the closure time of the end valve is normally longer than the stub water hammer wave return time. As a result, the diameter and length of connection stub for pressure-transducer should both be selected to be as small as possible. Another aspect that should be considered is the presence of air in the connection stub. If there is air trapped in the transducer connection, the transducer measurements can be completely wrong. So the transducer connection stub should not be installed in the upper side of the pipe to avoid the accumulation of air bubbles.

ACKNOWLEDGEMENTS

This work was partly supported by the National Natural Science Foundation of China (grant 51409197).

REFERENCES

Brunone, B. 1999 Transient test-based technique for leak detection in outfall pipes. *J. Water Resour. Plann. Manage.* **125** (5), 302–306.

Covas, D. & Ramos, H. 2010 Case studies of leak detection and location in water pipe systems by inverse transient analysis. *J. Water Resour. Plann. Manage.* **36** (2), 248–257.

Covas, D., Ramos, H. & Almeida, A. B. 2005 Standing wave difference method for leak detection in pipeline systems. *J. Hydraul. Eng.* **131** (12), 1106–1116.

Duan, H. F., Lee, P. J., Ghidaoui, M. S. & Tung, Y. K. 2011 Leak detection in complex series pipelines by using the system frequency response method. *J. Hydraul. Res.* **49** (2), 213–221.

Duan, H. F., Lee, P. J., Kashima, A., Lu, J. L., Ghidaoui, M. S. & Tung, Y. K. 2013 Extended blockage detection in pipes using the system frequency response: analytical analysis and experimental verification. *J. Hydraul. Eng.* **139** (7), 763–771.

Duan, H. F., Lee, P. J., Ghidaoui, M. S. & Tuck, J. 2014 Transient wave-blockage interaction and extended blockage detection in elastic water pipelines. *J. Fluids Struct.* **46** (4), 2–16.

Ferrante, M. & Brunone, B. 2003 Pipe system diagnosis and leak detection by unsteady-state tests. *1. Harmonic Analysis. Adv. Water Resour.* **26** (1), 95–105.

Gong, J. Z., Simpson, A. R., Lambert, M. F., Zecchin, A. C., Kim, Y. & Tijsseling, A. S. 2013 Detection of distributed deterioration in single pipes using transient reflections. *J. Pipeline Syst. Eng. Pract.* **4** (1), 32–40.

Kapelan, Z. S., Savic, D. A. & Walters, G. A. 2003 A hybrid inverse transient model for leakage detection and roughness calibration in pipe networks. *J. Hydraul. Res.* **41** (5), 481–492.

Lee, P. J., Vítkovský, J. P., Lambert, M. F., Simpson, A. R. & Liggett, J. A. 2005 Leak location using the pattern of the frequency response diagram in pipelines: a numerical study. *J. Sound Vib.* **284** (5), 1051–1073.

Lee, P. J., Vítkovský, J. P., Lambert, M. F., Simpson, A. R. & Liggett, J. A. 2007 Leak location in pipelines using the impulse response function. *J. Hydraul. Res.* **45** (5), 643–652.

Lee, P. J., Vítkovský, J. P., Lambert, M. F., Simpson, A. R. & Liggett, J. A. 2008 Discrete blockage detection in pipelines using the frequency response diagram: numerical study. *J. Hydraul. Eng.* **134** (5), 658–663.

Lee, P. J., Duan, H. F., Ghidaoui, M. S. & Karney, B. 2013 Frequency domain analysis of pipe fluid transient behavior. *J. Hydraul. Res.* **51** (6), 609–622.

Liggett, J. A. & Chen, L. C. 1994 Inverse transient analysis in pipe networks. *J. Hydraul. Eng.* **120** (8), 934–955.

Mpesha, W., Gassman, S. L. & Chaudhry, M. H. 2001 Leak detection in pipes by frequency response method. *J. Hydraul. Eng.* **127** (2), 134–147.

Sattar, A. M. & Chaudhry, M. H. 2008 Leak detection in pipelines by frequency response method. *J. Hydraul. Res.* **46** (S1), 138–151.

Stephens, M. L., Lambert, M. F. & Simpson, A. R. 2013 Determining the internal wall condition of a water pipeline in the field using an inverse transient. *J. Hydraul. Eng.* **139** (3), 310–324.

Vítkovský, J. P., Simpson, A. R. & Lambert, M. F. 2000 Leak detection and calibration using transients and genetic algorithms. *J. Water Resour. Plann. Manage.* **126** (4), 262–265.

Vítkovský, J. P., Lambert, M. F., Simpson, A. R. & Liggett, J. A. 2007 Experimental observation and analysis of inverse

transients for pipeline leak detection. *J. Water Resour. Plann. Manage.* **133** (6), 519–530.

Wang, X. J., Lambert, M. F., Simpson, A. R., Liggett, J. A. & Vítkovský, J. P. 2002 Leak detection in pipelines using the damping of fluid transients. *J. Hydraul. Eng.* **128** (7), 697–711.

Wang, X. J., Lambert, M. F. & Simpson, A. R. 2005 Detection and location of a partial blockage in a pipeline using damping of fluid transients. *J. Water Resour. Plann. Manage.* **131** (3), 244–249.

Wylie, E. B. & Streeter, V. L. 1993 *Fluid Transients in Systems.* Prentice Hall, Englewood Cliffs, NJ, USA.

First received 23 September 2017; accepted in revised form 15 January 2018. Available online 31 January 2018